Annals of Botany **132**: 895–907, 2023
https://doi.org/10.1093/aob/mcac157, available online at www.academic.oup.com/aob

ANNALS OF BOTANY
Founded 1887

PART OF A SPECIAL ISSUE ON CAM AT THE CROSSROADS

Photosynthesis and leaf structure of F_1 hybrids between *Cymbidium ensifolium* (C_3) and *C. bicolor* subsp. *pubescens* (CAM)

Yoko Yamaga-Hatakeyama[1], Masamitsu Okutani[1], Yuto Hatakeyama[2], Takayuki Yabiku[2], Tomohisa Yukawa[3] and Osamu Ueno[4,*]

[1]School of Agriculture, Kyushu University, Motooka, Nishi-ku, Fukuoka 819-0395, Japan, [2]Graduate School of Bioresource and Bioenvironmental Sciences, Kyushu University, Motooka, Nishi-ku, Fukuoka 819-0395, Japan, [3]Tsukuba Botanical Garden, National Museum of Nature and Science, Tsukuba, Ibaraki 305-0005, Japan and [4]Faculty of Agriculture, Kyushu University, Motooka, Nishi-ku, Fukuoka 819-0395, Japan
[*] *For correspondence: E-mail uenoos@agr.kyushu-u.ac.jp*

Received: 31 August 2022 Returned for revision: 17 November 2022 Editorial decision: 13 December 2022 Accepted: 16 December 2022

• **Background and aims** The introduction of crassulacean acid metabolism (CAM) into C_3 crops has been considered as a means of improving water-use efficiency. In this study, we investigated photosynthetic and leaf structural traits in F_1 hybrids between *Cymbidium ensifolium* (female C_3 parent) and *C. bicolor* subsp. *pubescens* (male CAM parent) of the Orchidaceae.
• **Methods** Seven F_1 hybrids produced through artificial pollination and *in vitro* culture were grown in a greenhouse with the parent plants. Structural, biochemical and physiological traits involved in CAM in their leaves were investigated.
• **Key results** *Cymbidium ensifolium* accumulated very low levels of malate without diel fluctuation, whereas *C. bicolor* subsp. *pubescens* showed nocturnal accumulation and diurnal consumption of malate. The F_1s also accumulated malate at night, but much less than *C. bicolor* subsp. *pubescens*. This feature was consistent with low nocturnal fixation of atmospheric CO_2 in the F_1s. The $\delta^{13}C$ values of the F_1s were intermediate between those of the parents. Leaf thickness was thicker in *C. bicolor* subsp. *pubescens* than in *C. ensifolium*, and those of the F_1s were more similar to that of *C. ensifolium.* This was due to the difference in mesophyll cell size. The chloroplast coverage of mesophyll cell perimeter adjacent to intercellular air spaces of *C. bicolor* subsp. *pubescens* was lower than that of *C. ensifolium*, and that of the F_1s was intermediate between them. Interestingly, one F_1 had structural and physiological traits more similar to those of *C. bicolor* subsp. *pubescens* than the other F_1s. Nevertheless, all F_1s contained intermediate levels of phosphoenolpyruvate carboxylase but as much pyruvate, Pi dikinase as *C. bicolor* subsp. *pubescens*.
• **Conclusions** CAM traits were intricately inherited in the F_1 hybrids, the level of CAM expression varied widely among F_1 plants, and the CAM traits examined were not necessarily co-ordinately transmitted to the F_1s.

Key words: CAM enzymes, CAM species, carbon isotope ratio, CO_2 exchange, C_3 species, *Cymbidium*, F_1 hybrids, inheritance, intercellular air space, leaf structure, malic acid accumulation, Orchidaceae.

INTRODUCTION

Crassulacean acid metabolism (CAM) is one of three major photosynthetic modes, together with C_3 and C_4 (Ehleringer and Monson, 1993). Its CO_2 assimilation mechanism is unique. In leaves of CAM plants, stomata are open at night and remain closed during much of the day. Thus, atmospheric CO_2 is mainly incorporated within leaves at night, when evaporative demand is low. It is initially fixed as oxaloacetate by phosphoenolpyruvate carboxylase (PEPC) and immediately converted to malate. The malate is temporarily stored as malic acid in the vacuoles. During the following day, it is decarboxylated within mesophyll cells, and released CO_2 is re-fixed by ribulose 1,5-bisphosphate carboxylase/oxygenase (Rubisco) in the Calvin cycle. This decarboxylation process concentrates CO_2 around Rubisco and reduces photorespiration (Osmond, 1978; Cushman and Bohnert, 1999; Schiller and Bräutigam, 2021; Winter and Smith, 2022).

Since CAM plants minimize evapotranspiration during the daytime, their water-use efficiency is much higher than in C_3 and C_4 plants (Winter *et al*., 2005). Reflecting this physiological trait, CAM plants are typically associated with arid environments (Winter, 1985; Ehleringer and Monson, 1993; Lüttge, 2004). In general, CAM plants have thick, succulent leaves composed of large mesophyll cells, which have vast vacuoles to store organic acids accumulated at night (Gibson, 1982; Lüttge, 2004; Nelson *et al*., 2005; Borland *et al*., 2018; Males, 2018). The intercellular air space (IAS) of mesophyll cells is often reduced in CAM leaves. This anatomical feature constrains internal conductance to CO_2 (Maxwell *et al*., 1997; Nelson and Sage, 2008; Cousins *et al*., 2020). It is noteworthy that the expression of CAM is very variable; for example, CAM species are classified into strong and weak CAM depending on the level of CAM expression (Winter, 2019).

The anatomical, biochemical and physiological traits of CAM plants are well characterized (Osmond, 1978; Lüttge, 2004; Winter, 2019; Schiller and Bräutigam, 2021), and knowledge of the molecular and genetic regulatory mechanisms of CAM expression is advanced (Cushman and Bohnert, 1999; Cushman *et al*., 2008; Yuan *et al*., 2020; Schiller and Bräutigam, 2021). On the other hand, improvement of the water-use efficiency of crops is a critical issue in agriculture under hotter and drier climates. The introduction of inducible CAM traits into C_3 crops by genetic engineering might improve their productivity in hot, water-limited fields (Borland *et al*., 2014; Yang *et al*., 2015; Töpfer *et al*., 2020; Yuan *et al*., 2020; Schiller and Bräutigam, 2021). However, many facets of the genetic regulation of CAM traits remain to be explored.

Hybridization studies using plants with different photosynthetic modes provide clues to the underlying genetic mechanisms (Björkman *et al*., 1971; Björkman, 1976; Brown and Bouton, 1993; Simpson *et al*., 2022). Early C_4 photosynthesis studies used crosses between C_3 and C_4 species of *Atriplex* (Björkman *et al*., 1971; Björkman, 1976). Subsequently, many hybridization studies have been undertaken using C_3, C_4, and C_3–C_4 intermediate species of various clades (Brown and Bouton, 1993; Ueno *et al*., 2003; Bang *et al*., 2009; Oakley *et al*., 2014; Simpson *et al*., 2022). However, few hybridization studies using C_3 and CAM species have been reported (reviewed in Brown and Bouton, 1993). Teeri and Overton (1981) reported that hybrids between C_3 (or weak CAM) and CAM species of the Crassulaceae had $\delta^{13}C$ values intermediate between the parent plants. More recently, a hybrid species, *Yucca gloriosa*, originated from a wild cross between a C_3 species, *Y. filamentosa*, and a CAM species, *Y. aloifolia*, of the Asparagaceae has been investigated (Heyduk *et al*., 2016, 2021). These studies report that the hybrid species exhibit intermediate C_3–CAM phenotypes of gas exchange, titratable acidity and leaf anatomy, suggesting that the CAM traits are transmitted to the progeny (Heyduk *et al*., 2016, 2021). These hybrids provide a useful system to explore the genetics of CAM. Further studies of hybrids between other C_3 and CAM species will be required for a deeper understanding of expression of CAM traits.

Here we report structural, biochemical and physiological traits in leaves of F_1 hybrids produced through artificial crossing between a C_3 and a CAM species of *Cymbidium*. The genus *Cymbidium* belongs to the Orchidaceae and has ~60 species with C_3 and CAM modes (Motomura *et al*., 2008). Their habitats are diverse, and species include terrestrial plants on forest floors, bark and humus epiphytes, and lithophytes. In this genus, CAM has evolved among epiphytes and lithophytes, which are compelled to live under water-limited environments (Motomura *et al*., 2008). It is possible to artificially produce hybrids between different *Cymbidium* species (Ogura-Tsujita *et al*., 2014). Here, we used *C. ensifolium* (subgenus *Jensoa*; Yukawa *et al*., 2002) as the C_3 female parent and *C. bicolor* subsp. *pubescens* (subgenus *Cymbidium*) as the CAM male parent. Their life forms also differ, reflecting the difference in photosynthetic mode: *C. ensifolium* is terrestrial and *C. bicolor* subsp. *pubescens* is epiphytic (Motomura *et al*., 2008).

The aim of this study was to characterize the structural, biochemical, and physiological traits involved in CAM in leaves of the F_1 hybrids so as to determine whether the CAM traits are transmitted to the F_1s.

MATERIALS AND METHODS

Plant materials and growth

Cymbidium ensifolium (L.) Sw. collected in Quezon, Luzon, the Philippines, was used as the female C_3 parent. *Cymbidium bicolor* subsp. *pubescens* Du Puy & P.J. Cribb, collected in Sarawak, Malaysia, was used as the male CAM parent. They were grown in a naturally lit greenhouse at the Tsukuba Botanical Garden, National Museum of Nature and Science, Tsukuba, Ibaraki, Japan, as described in Motomura *et al*. (2008). Seven F_1 hybrid plants (numbered 1–7) were produced from these parent plants by using artificial pollination and *in vitro* culture of collected seeds as described in Ogura-Tsujita *et al*. (2014). The same individual plant was used as female or male parent for all the F_1s. The pollinia of *C. bicolor* ssp. *pubescens* were placed on the stigma of *C. ensifolium* after flowering. All F_1 seeds were generated from the same artificial pollination event. The seeds were sown and subcultured aseptically in flasks (100–200 mL) containing 40–100 mL of culture medium. They were then transplanted into plastic pots filled with a 1:1 mixture of sphagnum moss and soil grown for ~5 years in the greenhouse. They were later transferred to the Faculty of Agriculture, Kyushu University, Fukuoka, Japan, together with three plants of *C. ensifolium* and three of *C. bicolor* subsp. *pubescens*. These parent plants differed from those used to generate the F_1s. All plants were grown in a growth chamber at the Biotron Application Center for a year at 25 °C and 70 % relative humidity under natural sunlight (Supplementary Data Fig. S1). The maximum photosynthetic photon flux density was ~1000 μmol m^{-2} s^{-1} at plant height. Plants were given 100 mL water per pot twice a week and fertilized with Hyponex nutrition solution (Hyponex Japan, Osaka, Japan; 100 mL of 1/1000 solution per pot) once a fortnight. The experiments were performed from July to September 2015. The day length was 12–14 h during this period.

Malate content

Malate content was determined in three fully expanded mature leaves per plant. Samples were collected from the middle region of the leaves, excluding the midrib and leaf margins, at 0500, 1100, 1700 and 2300 h. They were frozen immediately in liquid nitrogen and stored in a deep freezer (−80 °C) until analysis. The samples (0.2 g fresh weight) were ground in 0.5 mL of 5 % (v/v) $HClO_4$ and incubated for 20 min on ice. The homogenate was subsequently adjusted to pH 5 with 2 M KOH and centrifuged at 10 000 *g* for 10 min at 4 °C. The pellet was resuspended in 2 mL of distilled water and centrifuged again. The combined supernatants were used for determination of malate content according to the method of Möllering (1974). ΔMalate was calculated as the difference between the maximum and minimum contents.

Carbon dioxide exchange

The day/night pattern of CO_2 exchange was monitored to assess CAM expression in the parents and two F_1s (hybrids 3 and 4) with an LI-6400 portable photosynthesis system (Li-Cor Inc., Lincoln, NE, USA). An attached, fully expanded mature

leaf was clamped in the chamber. The space between the leaf and the chamber was sealed with handwork clay. Light within the chamber was provided by a 6400-02 LED Light Source (Li-Cor Inc.). The measurements were made at 25 °C leaf temperature, 65–75 % relative humidity, and a CO_2 concentration of 380 μL L^{-1}. The photosynthetic photon flux density during the light period was 500 μmol m^{-2} s^{-1}. The CO_2 uptake rate was monitored from 1720 h every 20 min for 24 h 40 min. The dark period was between 1800 and 0600 h.

Carbon isotope ratio

The leaf samples used for the measurement of fresh weight/dry weight (FW/DW) ratio were ground in a mortar with a pestle. Leaf powder (2 mg) was used to measure ^{12}C and ^{13}C contents. Carbon isotope ratios ($^{13}C/^{12}C$) were measured as described by Sato and Suzuki (2010) and expressed as $\delta^{13}C$ (‰) relative to the isotope ratio in the Pee Dee Belemnite standard (Ehleringer and Osmond, 1989).

Leaf thickness and FW/DW ratio

Leaf thickness was measured at the middle part between the leaf tip and base of ten fully expanded mature leaves per plant with Vernier callipers, excluding the midrib and leaf margins. Samples taken from the middle (~0.5 cm × 2 cm) of three leaves per plant were immediately weighed. Then they were air-dried at 80 °C for 2 days and weighed. The FW/DW ratio was calculated.

Leaf structure

Samples taken from the middle of three fully expanded mature leaves per plant, avoiding the midrib and margin (~2 mm × ~3 mm), between 0730 and 0800 h were fixed in 3 % (v/v) glutaraldehyde in 50 mM sodium phosphate buffer (pH 6.8) at room temperature for 2 h. They were then washed in phosphate buffer and post-fixed in 2 % OsO_4 in 50 mM sodium phosphate buffer for 2 h at room temperature. Samples were dehydrated through an acetone series, infiltrated with Quetol resin (Nishin EM, Tokyo, Japan) for 2 d, and then embedded in fresh Quetol resin. The resin was polymerized for 2 d at 70 °C. Transverse sections (1 μm thick) were cut with glass knives using an ultramicrotome (Porter-Blum MT-2B, Sorvall Inc., CT, USA), stained with 1 % toluidine blue O and observed under a light microscope (Biophot, Nikon, Tokyo, Japan).

Quantitative traits of mesophyll cells and their chloroplasts were measured using ImageJ software (National Institutes of Health, Bethesda, MD, USA; Supplementary Data Figs S2 and S3). The mesophyll cell size (planar area of mesophyll cell), proportion of IAS (percentage of cross-sectional area), and length of mesophyll surface exposed to IAS per unit area (L_{mes}/area) were determined according to the method of Nelson *et al.* (2005) (Supplementary Data Fig. S2). The sample areas analysed included both adaxial and abaxial sides of mesophyll. The number of chloroplasts per mesophyll cell was counted for ten adaxial and ten abaxial mesophyll cells in a transverse section. The chloroplast size (planar area of chloroplast) was also measured for five to eight of the adaxial and five to eight of the abaxial mesophyll cells used for measurement of the number of chloroplasts (three to five chloroplasts per cell). The chloroplast area per mesophyll cell area (Supplementary Data Fig. S3) was calculated using the chloroplast size, the number of chloroplasts per mesophyll cell, and the mesophyll cell size. The chloroplast coverage of mesophyll cell perimeter adjacent to the IAS (Supplementary Data Fig. S3) was measured for ten adaxial and ten abaxial mesophyll cells.

Stomatal density and guard cell length

Stomatal traits were measured in the middle part between the leaf tip and base of three fully expanded mature leaves per plant, avoiding the midrib and margin. The abaxial surface was painted with clear nail polish, because leaves of all plants lack adaxial stomata, as reported in *Cymbidium* species (Yukawa and Stern, 2002). The nail polish was air-dried, gently removed from the leaf surface on adhesive tape, and then set on a glass slide. The stomatal cast was observed under a light microscope. The stomatal density (SD), defined as number of stomata per unit leaf area, was determined in a field of 0.391 mm^2 at ×300 magnification with ten replications per leaf. The guard cell length (GL) of ten stomata selected randomly was measured at ×600 magnification with an ocular micrometer with three replications per leaf.

Western blotting of photosynthetic enzymes

Samples taken from the middle of fully expanded mature leaves, avoiding the midrib and margin, were immediately frozen in liquid nitrogen and stored in a deep freezer (−80 °C) until enzyme extraction. Leaves (1.0 g FW) were ground on ice using a pestle in a mortar containing 0.5 g of sea sand, 25 mg of polyvinylpyrrolidone and 1 mL of grinding medium composed of 100 mM HEPES·KOH (pH 8.0), 0.2 mM EDTA-2Na, 5 mM dithiothreitol, 1 mM phenylmethylsulphonyl fluoride, 0.1 % (w/v) leupeptin and 1 % (v/v) Triton X-100. The homogenates were filtered through gauze, the filtrates were centrifuged at 10 000 *g* for 10 min at 4 °C, and the supernatants were separated by sodium dodecyl sulphate–polyacrylamide gel electrophoresis and analysed by western blotting as described in Takao *et al.* (2022), using the antisera described in the next section. Soluble proteins [10 μg for PEPC and pyruvate, Pi dikinase (PPDK) and 2.5 μg for Rubisco large subunit (LSU)] were loaded in each lane. Protein contents were determined by use of a Bio-Rad (Richmond, CA, USA) protein assay kit.

Antisera used

Antisera raised against PEPC and PPDK from maize leaves and antiserum raised against Rubisco LSU from pea leaves were used for western blotting.

Statistical analysis

Data for malate content and structural traits of individual plants were obtained as means of three leaves per plant.

Using these mean values, means ± standard deviations of *C. ensifolium* (three plants), *C. bicolor* subsp. *pubescens* (three plants) and the F_1s (seven plants) were calculated. The carbon isotope ratios were represented by data obtained from one leaf per plant. Data were analysed in Statcel 4 software (OMS Publisher, Saitama, Japan). The significance of differences in structural and physiological traits was tested by ANOVA followed by Tukey–Kramer *post hoc* tests. $P < 0.05$ was considered statistically significant.

RESULTS

Day/night change in malate content

The malate content of *C. ensifolium* leaves was very low at all times of the day (Fig. 1A). The maximum value was 0.9 ± 1.1 μmol g FW^{-1} at 0500 h, and Δmalate (difference between the maximum and minimum values) was 1.1 ± 0.7 μmol g FW^{-1} (Table 1). In contrast, that of *C. bicolor* subsp. *pubescens* leaves was maximum at 0500 h, minimum at 1700 h and intermediate at 1100 and 2300 h (Fig. 1C). The mean malate contents of the seven F_1s were higher than in *C. ensifolium* but lower than in *C. bicolor* subsp. *pubescens*, except that that at 1700 h was similar to that in *C. bicolor* subsp. *pubescens* (Fig. 1B). Among the F_1s, hybrid 3 had a higher malate content at 0500 h than the others (Fig. 1D). ΔMalate was much higher in *C. bicolor* subsp. *pubescens* than in *C. ensifolium* and the F_1 mean (Table 1). Although Δmalate of the F_1s did not differ significantly from that of *C. ensifolium*, the former tended to be higher (Table 1). Among the F_1s, hybrid 3 had the highest value of Δmalate (Supplementary Data Table S1).

Carbon dioxide exchange pattern

The CO_2 exchange patterns in hybrids 3 and 4 were monitored as representatives of the F_1s, along with the parents (Fig. 2). *Cymbidium ensifolium* took up CO_2 only in the light period (Fig. 2A). *Cymbidium bicolor* subsp. *pubescens* took up a notable amount during the dark period (Fig. 2B); uptake increased rapidly with the change from dark to light, then decreased rapidly to nil, then became high again until the end of the light period. Hybrid 3 showed a diurnal pattern of CO_2 uptake intermediate between those of the parents: it took up a small amount of CO_2 between 0000 and 0500 h, and took up less in the daytime than *C. ensifolium* but more than *C. bicolor* subsp. *pubescens* (Fig. 2C). Hybrid 4 showed a diurnal pattern that was similar to that in *C. ensifolium* but took up CO_2 weakly around midnight (Fig. 2D).

Carbon isotope ratio

Cymbidium bicolor subsp. *pubescens* leaves had higher $\delta^{13}C$ values than *C. ensifolium* leaves (Table 1). The mean $\delta^{13}C$ of the seven F_1s was intermediate. The $\delta^{13}C$ of hybrid 3 approached that of *C. bicolor* subsp. *pubescens* (Fig. 3A; Supplementary

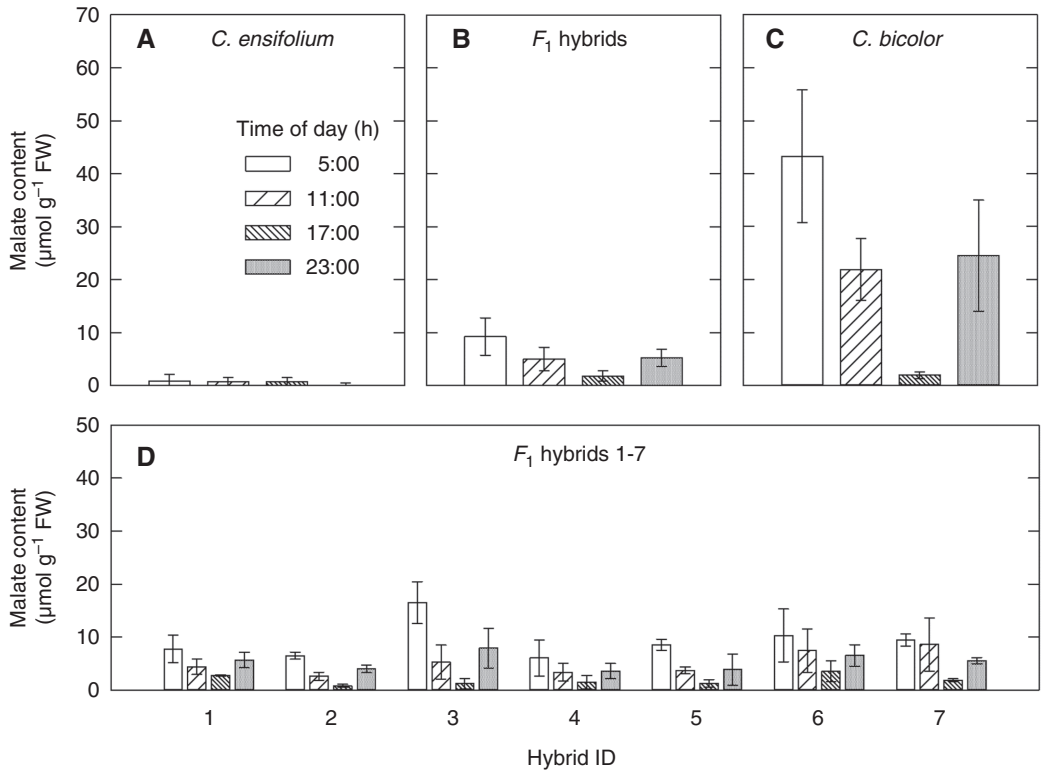

FIG. 1. Diel patterns of malate content (mean ± standard deviation) in leaves of (A) *C. ensifolium* ($n = 3$), (B) F_1 hybrids ($n = 7$), (C) *C. bicolor* subsp. *pubescens* ($n = 3$) and (D) individual F_1s (means of three measurements).

TABLE 1. *Physiological and structural traits in leaves of* C. ensifolium, C. bicolor *subsp.* pubescens, *and their* F_1 *hybrids*

Traits	***C. ensifolium***	***F*** $_1$ hybrids	***C. bicolor*** subsp. ***pubescens***
ΔMalate (μmol g FW^{-1})	1.1 ± 0.7b	7.9 ± 3.6b	41.3 ± 12.0a
$\delta^{13}C$ (‰)	−30.3 ± 1.4a	−25.6 ± 1.6b	−21.9 ± 0.9c
Leaf thickness (mm)	0.42 ± 0.01b	0.50 ± 0.12b	1.37 ± 0.05a
FW/DW ratio	4.10 ± 0.48c	6.31 ± 0.72b	7.83 ± 0.80a
Mesophyll cell size (μm^2)	725.8 ± 50.0c	1957.4 ± 243.2b	3497.7 ± 263.2a
IAS (%)	9.4 ± 1.0a	5.6 ± 0.4b	4.3 ± 1.2b
L_{mes}/area (μm^{-1})	0.058 ± 0.004a	0.028 ± 0.001b	0.019 ± 0.002c
Chloroplast size (μm^2)	28.2 ± 3.3a	26.4 ± 2.8a	13.3 ± 1.6b
Chloroplast area per mesophyll cell area (%)	23.2 ± 8.6a	11.8 ± 0.7b	5.1 ± 0.8b
Chloroplast coverage of mesophyll cell perimeter adjacent to IAS (%)	85.9 ± 5.1a	78.2 ± 2.5b	60.5 ± 3.2c
Stomatal density (no. per mm^2)	121.9 ± 8.2a	81.5 ± 7.7b	86.2 ± 9.5b
Guard cell length (μm)	31.6 ± 1.1a	24.0 ± 1.4b	20.3 ± 0.9c

Values are means ± standard deviation of three *C. ensifolium* plants, seven F_1 plants and three *C. bicolor* subsp. *pubescens* plants. Different letters indicate a significant difference at $P < 0.05$.

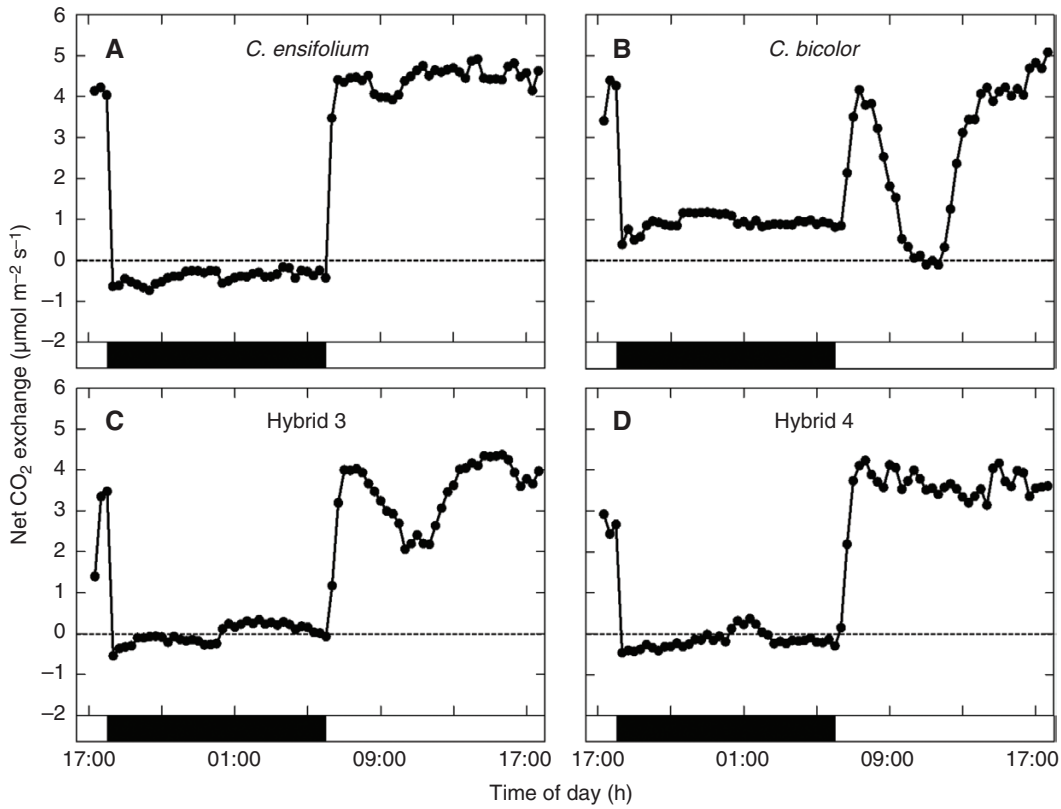

FIG. 2. Net CO_2 exchange in leaves of (A) *C. ensifolium*, (B) *C. bicolor* subsp. *pubescens*, (C) hybrid 3, and (D) hybrid 4 during 12 h of darkness and 12 h of light.

Data Table S1). There was a positive relationship between Δmalate and $\delta^{13}C$ values (Fig. 3A).

Leaf thickness and FW/DW ratio

Cymbidium bicolor subsp. *pubescens* had thicker leaves than *C. ensifolium* and the F_1 mean, but there was no significant difference between *C. ensifolium* and the F_1s (Table 1). Among the F_1s, hybrid 3 had the thickest leaves (Fig. 3B; Supplementary Data Table S1). The FW/DW ratio of leaves was much higher in *C. bicolor* subsp. *pubescens* than in *C. ensifolium*, and the F_1 mean was intermediate (Table 1). The parents and F_1s had a strong positive relationship between Δmalate and leaf thickness (Fig. 3B) and a weak and not significant positive relationship between Δmalate and FW/DW (Fig. 3C).

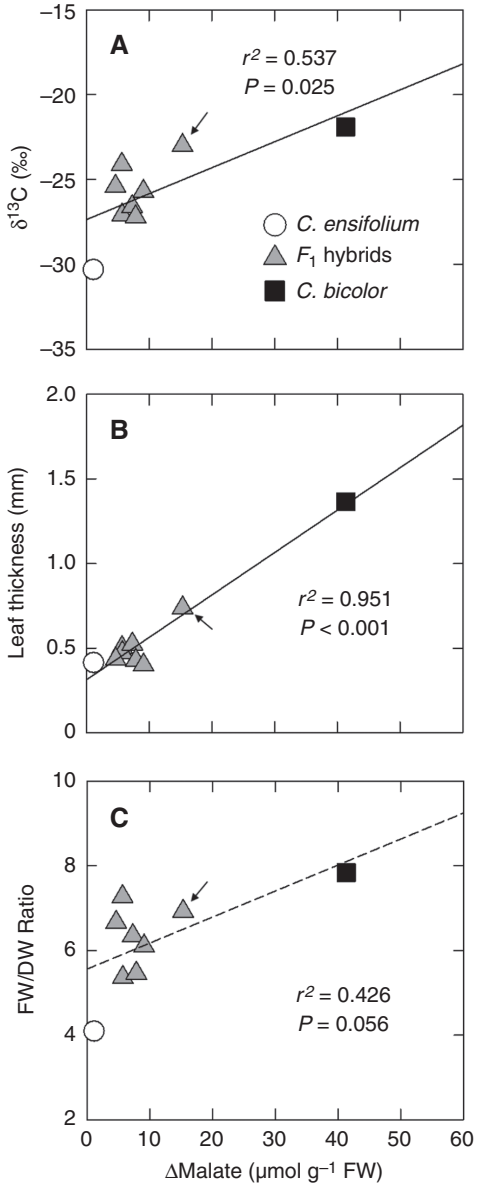

FIG. 3. Relationships between Δmalate and (A) $\delta^{13}C$ values, (B) leaf thickness and (C) FW/DW ratio in leaves of *C. ensifolium*, *C. bicolor* subsp. *pubescens*, and their F_1 hybrids. Arrows show values of hybrid 3. The dashed line in (C) is a regression line with a non-significant *P* value ($0.05 < P < 0.1$).

Leaf structure

In *C. ensifolium* leaves, all mesophyll cells were round (Fig. 4A). However, those near both epidermises were smaller than the rest. In *C. bicolor* subsp. *pubescens* leaves, the mesophyll was tightly arranged as elongated cells, except for small round cells near the abaxial epidermis (Fig. 4B). Mesophyll cells were more elongated in the adaxial mesophyll than in the abaxial mesophyll. There were few IASs between the adaxial mesophyll cells. Except in the leaves of hybrid 3 (Fig. 4E), leaves of all F_1 s had anatomical structures similar to those of *C. ensifolium* but with a slight trend of elongation in the adaxial mesophyll cells (Fig. 4C, D, F–I). Hybrid 3 leaves clearly had a mixed mesophyll structure with features of both parents: elongated adaxial mesophyll cells but round abaxial cells (Fig. 4E).

Quantitative analysis showed that the size of mesophyll cells was much larger in *C. bicolor* subsp. *pubescens* than in *C. ensifolium*, and the F_1 mean was intermediate (Table 1). As expected, the mesophyll cell size of hybrid 3 was largest among seven F_1s (Fig. 5A; Supplementary Data Table S2). The parents and F_1s had a strong positive relationship between Δmalate and mesophyll cell size (Fig. 5A). *Cymbidium ensifolium* had more IAS than *C. bicolor* subsp. *pubescens* and the F_1 mean, but there was no significant difference between *C. bicolor* subsp. *pubescens* and the F_1 mean (Table 1). There was no significant relationship between Δmalate and percentage of IAS (Fig. 5B). On the other hand, *C. ensifolium* had longer L_{mes}/area than *C. bicolor* subsp. *pubescens*, and the F_1 mean was intermediate (Table 1). There was no significant relationship between Δmalate and L_{mes}/area (Fig. 5C).

Cymbidium bicolor subsp. *pubescens* had smaller chloroplasts than *C. ensifolium* and the F_1 mean, but there was no significant difference between *C. ensifolium* and the F_1s (Table 1). The chloroplast size of hybrid 3 was almost the same as that of *C. ensifolium* (Fig. 5D; Supplementary Data Table S2). The chloroplast area per mesophyll cell area was greater in *C. ensifolium* than in *C. bicolor* subsp. *pubescens* and the F_1 mean (Table 1). There were weak, non-significant negative relationships between Δmalate and chloroplast size and between Δmalate and chloroplast area per mesophyll cell area (Fig. 5D, E). The chloroplast coverage of mesophyll cell perimeter adjacent to IAS was greater in *C. ensifolium* than in *C. bicolor* subsp. *pubescens*, and the F_1 mean was intermediate (Table 1). There was a strong negative relationship between Δmalate and chloroplast coverage of mesophyll cell perimeter adjacent to IAS ($P < 0.01$; Fig. 5F).

Stomata

Both SD and GL were greater in *C. ensifolium* than in *C. bicolor* subsp. *pubescens* (Table 1). The mean SD of the seven F_1s did not differ from that of *C. bicolor* subsp. *pubescens* (Table 1). Among the F_1s, hybrid 3 had the lowest SD (Fig. 6A; Supplementary Data Table S1). The mean GL of the seven F_1s was intermediate between those of the parents but was close to that of *C. bicolor* subsp. *pubescens* (Table 1). There was no significant relationship between Δmalate and SD (Fig. 6A). However, there was a weak, non-significant negative relationship between Δmalate and GL (Fig. 6B).

Western blot analysis of photosynthetic enzymes

We found PEPC bands in leaves of all plants examined (Fig. 7). Those in *C. bicolor* subsp. *pubescens* were clearly denser than the rest, and those in the F_1s were slightly denser than those in *C. ensifolium*. The PPDK bands in *C. bicolor* subsp. *pubescens* and all F_1s had comparable density (Fig. 7). Those in *C. ensifolium*, however, were weak or absent. Rubisco LSU bands occurred in leaves of all plants examined (Fig. 7). Those in *C. ensifolium* were somewhat denser than those in *C. bicolor* subsp. *pubescens*. Those in the F_1s varied in density among

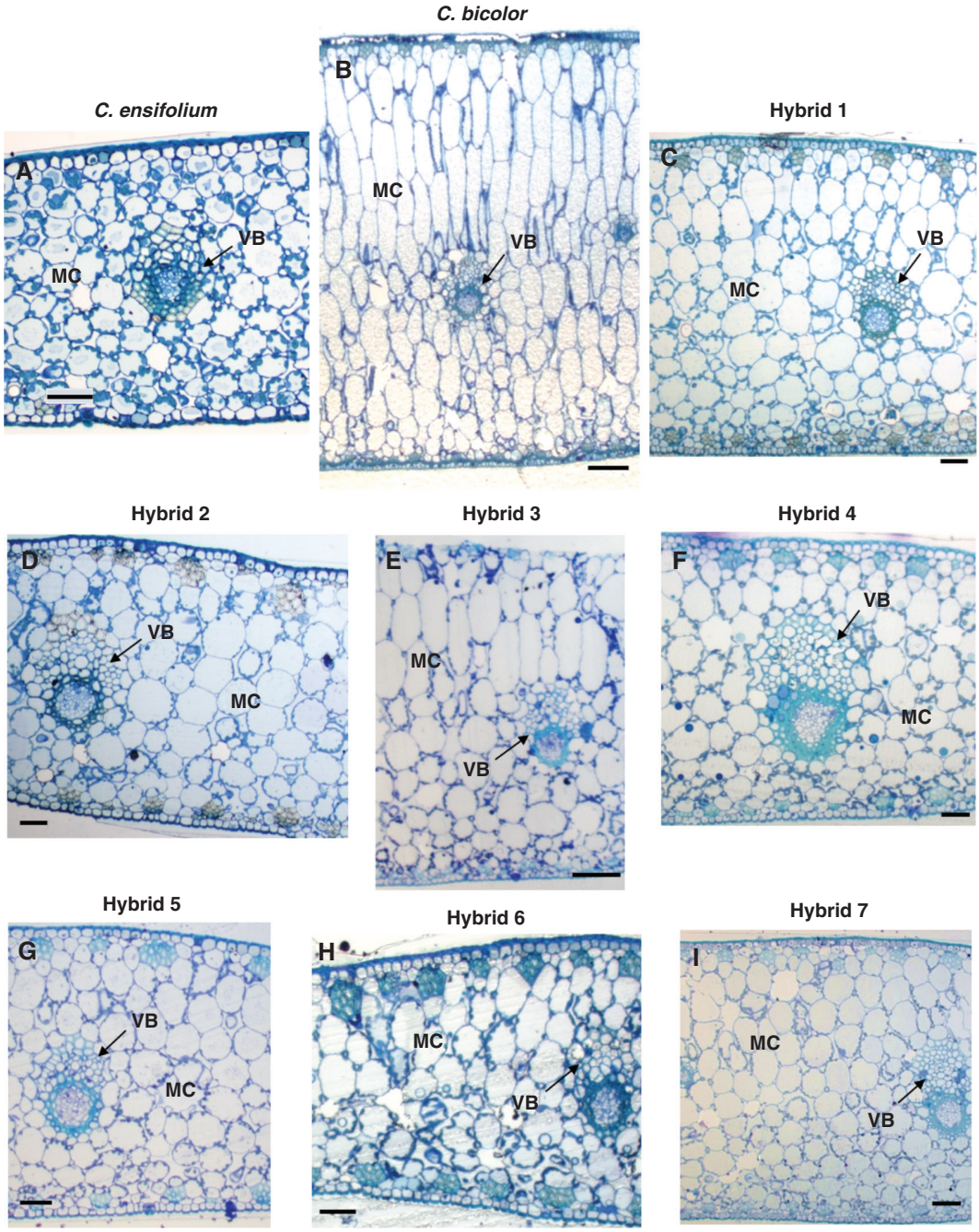

FIG. 4. Inner structure of leaves of (A) *C. ensifolium*, (B) *C. bicolor* subsp. *pubescens* and (C–I) F_1 hybrids 1–7. MC, mesophyll cell, VB, vascular bundle. Scale bars in (B) and (E) = 100 μm; in other panels = 50 μm.

plants within the range of the parental sizes (Fig. 7). That of hybrid 3 was weakest among all F_1s.

DISCUSSION

Photosynthetic traits

Our results confirm that *C. ensifolium* plants had very low levels of malate without diurnal fluctuation (Fig. 1A) and C_3-like $\delta^{13}C$ values (Table 1), and fixed atmospheric CO_2 only in the daytime (Fig. 2A), as is typical of C_3 plants. The *C. bicolor* subsp. *pubescens* plants showed the day/night pattern of CO_2 uptake typical of CAM (Fig. 2C) but lower CO_2 uptake at night than in strong CAM plants (Winter, 2019). Their $\delta^{13}C$ value (–21.9‰) was also lower than those in strong CAM plants and lay at the higher end of the range of values in C_3 plants (Ehleringer and Osmond, 1989; Silvera *et al.*, 2005; Motomura *et al.*, 2008). It is well known that $\delta^{13}C$ values of weak CAM plants often overlap those of C_3 plants (Winter and Holtum, 2002; Silvera *et al.*, 2005; Motomura *et al.*, 2008).

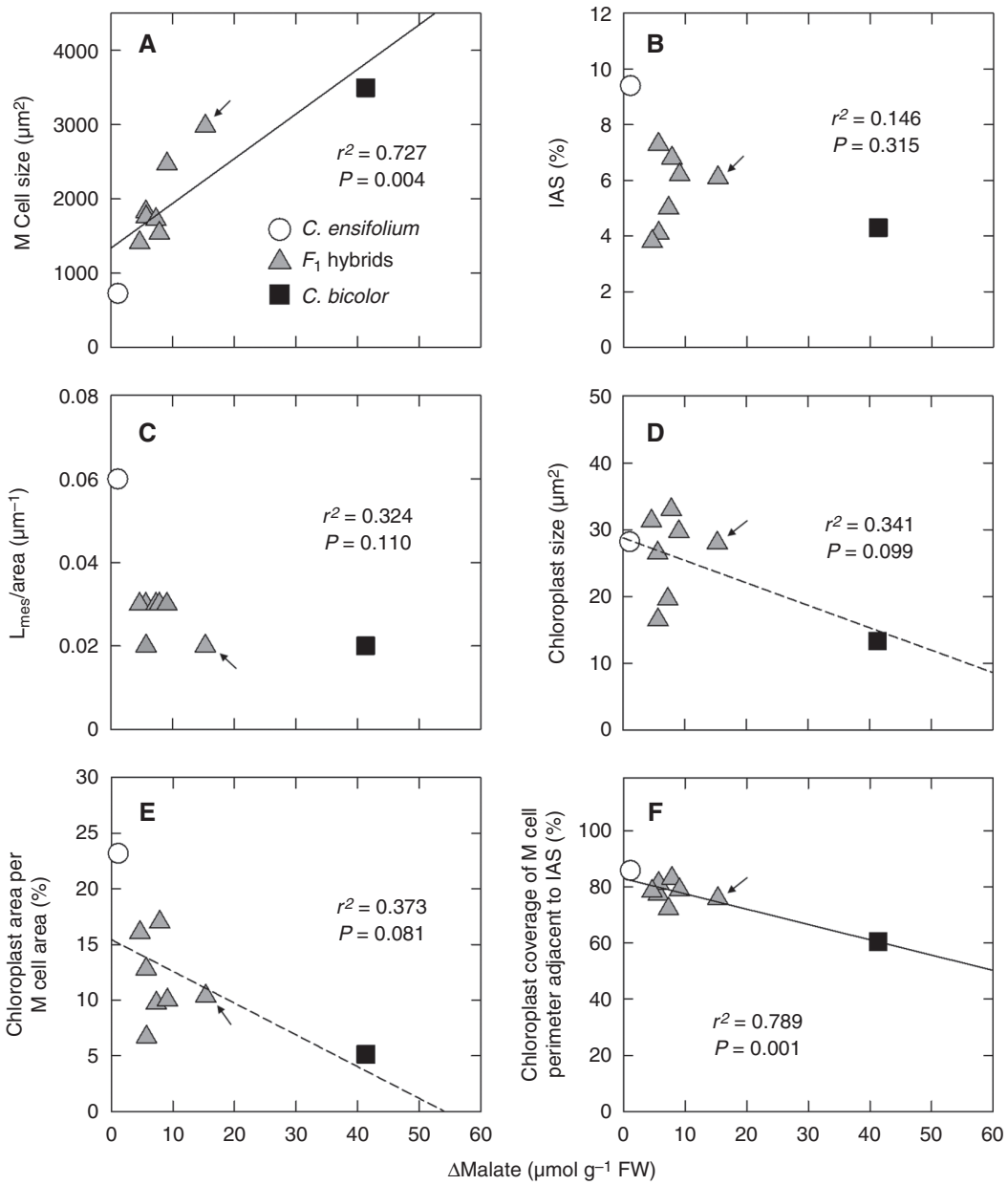

FIG. 5. Relationships between Δmalate and (A) mesophyll cell size, (B) proportion of IAS, (C) L_{mes}/area, (D) chloroplast size, (E) chloroplast area per mesophyll cell area and (F) chloroplast coverage of cell perimeter adjacent to IAS in leaves of *C. ensifolium*, *C. bicolor* subsp. *pubescens* and their F_1 hybrids. M, mesophyll. Arrows show values of hybrid 3. Regression lines with non-significant *P* values ($0.05 < P < 0.1$) are shown by dashed lines.

The malate content at the end of night (0500 h) in *C. bicolor* subsp. *pubescens* (Fig. 1C) was somewhat higher than that reported previously (Motomura *et al*., 2008), although the plants differed from those examined in the previous study. Although there are some differences in data, we consider that our *C. bicolor* subsp. *pubescens* plants express weaker CAM activity than those in the previous study, on the basis of the CO_2 exchange pattern and $\delta^{13}C$ values. The expression of CAM is affected by environmental conditions during growth (Lüttge, 2004; Winter, 2019). It seems likely that differences in the growth conditions (temperature and water supply) between the present and previous studies caused the modification of CAM expression in *C. bicolor* subsp. *pubescens*.

Although there was no significant difference in Δmalate between the F_1s and the C_3 parent *C. ensifolium*, values in the former tended to be higher than those in the latter (Table 1). Furthermore, the malate content of all F_1s had maximum values at 0500 h and minimum values at 1700 h, as in the CAM parent *C. bicolor* subsp. *pubescens* (Fig. 1). This night/day pattern of malate accumulation is characteristic of CAM plants but not of C_3 plants (Winter and Smith, 2022). These facts verify that the F_1s are derived from hybridization between C_3 and CAM species, and significant biochemical traits of CAM were transferred to the F_1s. Among the seven F_1s, hybrid 3 had the highest Δmalate (15.3 μmol g FW^{-1}), although this was lower than the midpoint between the parents (21 μmol g FW^{-1}). The $\delta^{13}C$

values of all F_1s lay between those of the parents, but that of hybrid 3 was closest to that of *C. bicolor* subsp. *pubescens* (Fig. 3A). These data suggest differences in the expression level of CAM among the F_1s. It is unlikely that the higher expression of CAM in hybrid 3 was caused by differences in growth conditions, because we saw a similar trend in the F_1s in our preliminary experiment in 2014 (Supplementary Data Fig. S4). The CO_2 exchange pattern during the day confirmed a weaker CAM in hybrid 3 than in *C. bicolor* subsp. *pubescens*, as indicated by lower CO_2 uptake at night (phase I; Osmond, 1978) and higher CO_2 uptake in the daytime (phase III) than in *C. bicolor* subsp. *pubescens* (Fig. 2). On the other hand, that in hybrid 4 was similar to that in *C. ensifolium* but showed a slight CO_2 uptake in phase I (Fig. 2). Taken together, these results suggest that the photosynthetic traits of CAM were weakly transmitted to the F_1s, with variation among individual plants. Whether the expression of CAM traits in the F_1s is enhanced under drought stress remains a question.

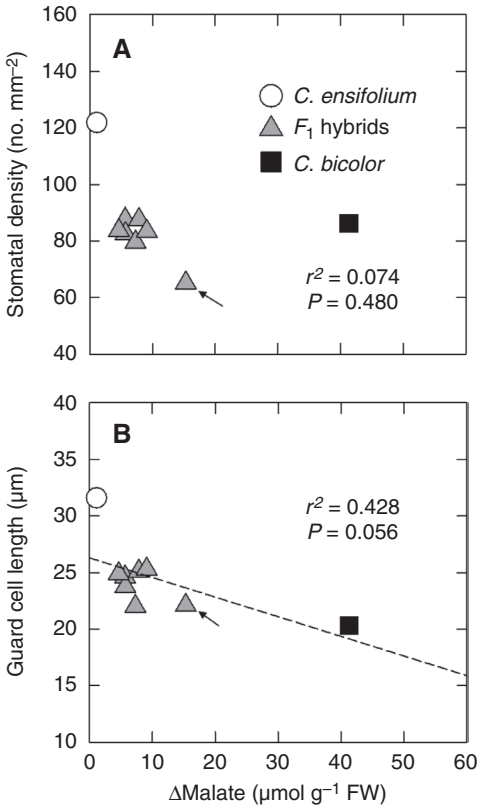

FIG. 6. Relationships between Δmalate and (A) stomatal density and (B) guard cell length in leaves of *C. ensifolium*, *C. bicolor* subsp. *pubescens* and their F_1 hybrids. Arrows show values of hybrid 3. The dashed line in (B) is a regression line with a non-significant P value ($0.05 < P < 0.1$).

Expression of photosynthetic enzymes

There are different isoforms of PEPC in plants: C_4, CAM and non-photosynthetic (Chollet *et al*., 1996; Izui *et al*., 2004). The CAM isoform of PEPC is post-translationally activated at night by a protein kinase (Nimmo, 2000; Schiller and Bräutigam, 2021). As expected, *C. bicolor* subsp. *pubescens* contained abundant PEPC. *Cymbidium ensifolium* also contained notable PEPC (Fig. 7). As *C. ensifolium* has C_3 photosynthetic traits, this PEPC would be involved not in photosynthetic function but in other functions, such as anaplerotic reactions to replenish biosynthetic precursors for the tricarboxylic acid cycle (Chollet *et al*., 1996; Izui *et al*., 2004). A study of PEPC isoforms in orchids reported that C_3 orchid species possess non-photosynthetic PEPC isogenes, whereas the strong and weak CAM orchid species have both CAM-specific and non-photosynthetic PEPC isogenes (Silvera *et al*., 2014). The F_1s contained slightly more PEPC than *C. ensifolium* but less than *C. bicolor* subsp. *pubescens* (Fig. 7). Although it is unknown whether all of the PEPC in the F_1s is involved in CAM, it appears that these amounts of PEPC approximately correlate with the difference in CAM activity between *C. bicolor* subsp. *pubescens* and the F_1s, indicating that some PEPC is responsible for the weak CAM function in F_1s. We do not know why hybrid 3 contained PEPC at similar levels to other F_1s. The F_1s between C_4 and C_3 species of *Atriplex* have PEPC enzymatic properties intermediate between the parents (Björkman, 1976). The PEPC in these F_1s remains to be characterized.

In CAM photosynthesis, Rubisco is involved in CO_2 fixation in phases II–IV (Osmond, 1978; Maxwell *et al*., 1999; Schiller and Bräutigam, 2021). The amount of Rubisco LSU protein was greater in *C. ensifolium* than in *C. bicolor* subsp. *pubescens* (Fig. 7). The amount in the F_1s tended to be lower than that in *C. ensifolium*, although with wide variation (Fig. 7). Rubisco LSU is encoded in the chloroplast genome and determines the kinetic properties of Rubisco (Hudson *et al*., 1990). Thus, a reciprocal hybridization study will be required to understand the genetic regulation of Rubisco LSU.

The pattern of PPDK content differed considerably from that of PEPC (Fig. 7). *Cymbidium ensifolium* accumulated little or no PPDK, whereas the F_1s accumulated almost as much as *C. bicolor* subsp. *pubescens* (Fig. 7). CAM is divided into two

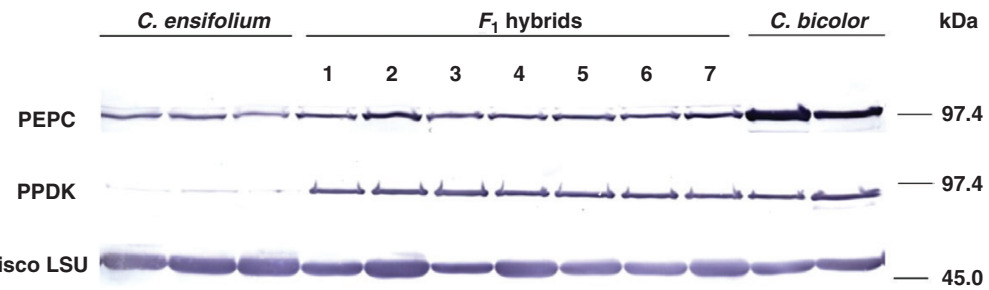

FIG. 7. Western blots of PEPC, PPDK and Rubisco LSU in leaves of *C. ensifolium*, *C. bicolor* subsp. *pubescens* and their F_1 hybrids.

subtypes on the basis of the malate decarboxylation process: malic enzyme (ME) and phosphoenolpyruvate carboxykinase (PCK) types (Dittrich *et al*., 1973; Dittrich, 1976). The leaves of *C. bicolor* subsp. *pubescens* have high activities of NADP-ME and NAD-ME but lack PCK activity, indicating that this species uses ME-type CAM (Motomura *et al*., 2008). In ME-type CAM, malate is decarboxylated by NADP-ME and NAD-ME, generating pyruvate + CO_2. Subsequently, pyruvate is phosphorylated to PEP by PPDK and is conserved in gluconeogenesis (Holtum and Osmond, 1981; Kondo *et al*., 2000; Dever *et al*., 2015). The patterns of PPDK content in the two parents and F_1s suggest that the high expression of PPDK in the F_1s is due to the transfer of the *PPDK* gene from the CAM parent, *C. bicolor* subsp. *pubescens*. On the other hand, the high accumulation of PPDK in the F_1s may be a waste of nitrogen, since it would be excessive for the operation of very weak CAM.

Relationships between leaf structural traits and CAM expression

Cymbidium bicolor subsp. *pubescens* had thicker leaves and a higher FW/DW ratio than *C. ensifolium* (Table 1), indicative of the development of succulence in the former. Leaf thickening was brought about by cell elongation, especially in the palisade mesophyll (Fig. 4B; Yukawa and Stern, 2002). A positive relationship between increased nocturnal CO_2 uptake and the development of palisade mesophyll cells, which results in thicker leaves, has been found in leaves of C_3, C_3–CAM intermediate and CAM species of *Clusia* (Barrera-Zambrano *et al*., 2014; Borland *et al*., 2018; Lujan *et al*., 2022). This anatomical feature may accommodate the increased energetic requirements of CAM by improving light harvesting (Barrera-Zambrano *et al*., 2014). *Cymbidium ensifolium* occurs mainly in the understorey of rainforest in tropical, subtropical and warm regions, whereas *C. bicolor* ssp. *pubescens* grows in the canopy site of tropical forest (Motomura *et al*., 2008). The difference in habitat light environments between the two *Cymbidium* species may relate to the mesophyll structure in association with CAM expression. There was a strong positive correlation between Δmalate and leaf thickness in the parents and F_1s (Fig. 3B), but only a positive trend between Δmalate and FW/DW (Fig. 3C). However, the leaf thicknesses of all F_1s except hybrid 3 approached that of *C. ensifolium*, whereas the FW/DW ratios were scattered between those of the parents. These results indicate that FW/DW in *Cymbidium* leaves does not simply correlate with leaf thickness.

The quantitative analysis indicated that the structural traits of mesophyll cells and their chloroplasts differed greatly between *C. ensifolium* (C_3) and *C. bicolor* subsp. *pubescens* (CAM). The latter species had larger mesophyll cells (Fig. 5A), a lower proportion of IAS (Fig. 5B) and shorter L_{mes}/area (Fig. 5C). These data corresponded well with those found in previous comparative studies on leaf structure of C_3 and CAM species (Gibson, 1982; Fioretto and Alfani, 1988; Kondo *et al*., 1998; Nelson *et al*., 2005; Nelson and Sage, 2008; Heyduk *et al*., 2016; Males, 2018; Herrera, 2020). It is considered that the reduced IAS and L_{mes}/area of mesophyll cells are associated with reduced CO_2 conductance in CAM leaves (Maxwell *et al*., 1997; Nelson *et al*., 2005; Nelson and Sage, 2008; Cousins *et al*., 2020). In the parents and F_1s there was a positive relationship between Δmalate and mesophyll cell size (Fig. 5A) and the F_1s were situated between the parents (Table 1). As expected, the value of hybrid 3 approached that of the CAM parent. In the parents and F_1s there was a positive relationship between mesophyll cell size and leaf thickness (r^2 = 0.630; P = 0.011) and a negative relationship between mesophyll cell size and L_{mes}/area (r^2 = 0.615; P = 0.012). Thus, it appears that there are relationships among leaf thickness, mesophyll cell size and L_{mes}/area. Meanwhile, the PEPC content of leaves did not differ among the F_1s (Fig. 7), but hybrid 3, having larger mesophyll cells, showed greater Δmalate than other F_1s (Fig. 5A). These facts suggest that mesophyll cell size may be one of the factors limiting the operation of the CAM cycle in the F_1s.

As far as we know, there are almost no quantitative data on chloroplasts of CAM plants. Our study indicated that *C. bicolor* subsp. *pubescens* had smaller chloroplasts than *C. ensifolium* and the F_1 mean. Although the values of F_1s were greatly varied, there was no significant difference between *C. ensifolium* and the F_1 mean (Table 1, Fig. 5D). The chloroplast area per mesophyll cell area of *C. bicolor* subsp. *pubescens* was much smaller than that of *C. ensifolium* (Table 1). Stata *et al.* (2014) reported the chloroplast area per mesophyll cell area to be 21–31 % and 12–17 % for C_3 and C_4 species, respectively. The value for *C. ensifolium* was similar to those of the C_3 species, and that of *C. bicolor* subsp. *pubescens* was much smaller than those of the C_4 species. The lowest value in the CAM parent would be mainly owing to the vast vacuoles in the mesophyll cells.

In C_3 plants, Rubisco occurs in chloroplasts of mesophyll cells. Thus, it would be essential for C_3 plants to distribute chloroplasts along the IAS of mesophyll, because this positioning would facilitate the fixation of atmospheric CO_2 (Evans and Loreto, 2000; Cousins *et al*., 2020). In contrast, in C_4 plants the primary carboxylase PEPC occurs in the cytosol of mesophyll cells, whereas their chloroplasts lack Rubisco (Hatch, 1987; Ueno, 1998). Thus, the positioning of chloroplasts adjacent to IAS in C_3 plants would not be requisite for C_4 plants (Nelson *et al*., 2005; Stata *et al*., 2014). In CAM plants, PEPC and Rubisco are localized in the cytosol and chloroplasts of mesophyll cells, respectively (Kondo *et al*., 1998; Cushman and Bohnert, 1999; Schiller and Bräutigam, 2021). CAM plants fix atmospheric CO_2 predominately by PEPC in phase II and by Rubisco in phase IV (Osmond *et al*., 1978; Roberts *et al*., 1997; Maxwell *et al*., 1999). The chloroplast coverage of mesophyll cell perimeter adjacent to the IAS is considered a structural index to evaluate mesophyll conductance (Evans and Loreto, 2000; Stata *et al*., 2014). Stata *et al*. (2014) reported values of ~90 and 40 % for C_3 and C_4 species, respectively. The value for *C. ensifolium* was similar to that for C_3 species, whereas the value for *C. bicolor* subsp. *pubescens* was intermediate between those for C_3 and C_4 species (Table 1). The intermediate value in *C. bicolor* subsp. *pubescens* may reflect the use of two carboxylases in mesophyll cells. In the parents and F_1s there was a strong negative relationship between Δmalate and the chloroplast coverage of mesophyll cell perimeter adjacent to the IAS (Fig. 5F), suggesting that this structural trait may be involved in CAM physiology. In the present study, we fixed leaf tissues in the early morning (phase II). Thus, it remains unknown whether the positioning of chloroplasts changes with the day/night cycle of CAM. Under combined light and water stress, a day/night change in chloroplast positioning has been reported in succulent CAM plants (Kondo *et al*., 2004).

In general, more succulent species have lower SD than less succulent species (Gibson, 1982; Lüttge, 2004). The lower SD seems to favour the survival of succulent CAM species in dry environments. However, the relationships between GL and succulence or CAM in leaves are more complex. In bifacial leaves of *Senecio*, including CAM cycling and obligate CAM species, there is a negative correlation between SD and GL (Fioretto and Alfani, 1988). This relationship of stomatal traits is also found in species of other genera (Franks *et al*., 2009; Tsutsumi *et al*., 2017) and among cultivars of a species (Yabiku and Ueno, 2017), irrespective of the photosynthetic mode. In *Clusia* species, SD is negatively correlated and stomatal pore area is positively correlated with nocturnal CO_2 uptake rate (Barrera-Zambrano *et al*., 2014). In the *Cymbidium* plants examined here, GL tended to decrease with increasing Δmalate (Fig. 6B), but there was no relationship between SD and Δmalate (Fig. 6A). Stomatal density in F_1s was closer to that of the CAM parent, but hybrid 3 had the lowest SD. This pattern in the F_1s is clearly different from that of leaf thickness. Therefore, the increase in mesophyll cell size resulting in thicker leaves and the decrease in stomatal size (GL) may be regulated by different genetic mechanisms. In general, cell size, including that of guard cells, seems to be under common genetic control, probably via genome size (Beaulieu *et al*., 2008).

Inheritance of CAM and leaf anatomical traits in Cymbidium F_1 *hybrids*

As a whole, the photosynthetic traits (Δmalate and CO_2 exchange) of the F_1s approached those of the C_3 parent rather than the CAM parent. However, PPDK accumulated in the *Cymbidium* F_1s to levels similar to those in the CAM parent, whereas the $\delta^{13}C$ values of most F_1s were midway between those of the parents. On the other hand, the structural traits of leaves were also intricately inherited in the F_1s; some traits were intermediate between those of the parents, whereas other traits approached those of either parent. These results indicate that the inheritance of CAM traits was complex, and the traits were not necessarily co-ordinately transmitted to the F_1s. As exemplified by hybrid 3, the level of CAM expression varied widely among F_1s. It is interesting to note that, in the C_3 + CAM hybrid species *Yucca gloriosa* also, considerable genotypic variations have been found in gas exchange and acid accumulation patterns (Heyduk *et al*., 2021), although this hybrid must also be considered to be derived from natural hybridization. To determine whether a maternal effect (chloroplast and mitochondrial DNA control) is involved in the expression of CAM traits, we will need reciprocal F_1s. Analyses of advanced generations beyond the F_1 would also be required for a deeper understanding of the inheritance of components of CAM photosynthesis and leaf anatomy, and an attempt at production of F_2 plants has been made. It seems that the C_3 + CAM hybrid species of *Yucca* investigated by Heyduk *et al.* (2016) originated from the parent with stronger CAM expression than the CAM parent *C. bicolor* subsp. *pubescens* used in this study. This *Yucca* hybrid showed higher nocturnal CO_2 uptake than in the F_1s of *Cymbidium*. This suggests that the degree of CAM expression in hybrids would be affected by those of the parents used. Meanwhile, *C. ensifolium* and *C. bicolor* belong to different clades of *Cymbidium* (Yukawa *et al.*, 2002; Motomura *et al.*, 2008). Further studies with F_1s generated from more closely related C_3 and CAM species of *Cymbidium* may also provide different patterns of CAM expression.

The performance of CAM does not require the differentiation of two types of photosynthetic cell that is a prerequisite for C_4 photosynthesis. However, CAM leaves have large succulent mesophyll cells differing from those of C_3 and C_4 leaves. The strict relationship between leaf succulence and the degree of CAM expression remains to be elucidated. Our understanding of the cellular developmental mechanism of CAM leaves will also be needed for engineering of the CAM traits in C_3 crops, together with those of the complex circadian control of cellular metabolism and stomatal movement.

SUPPLEMENTARY DATA

Supplementary data are available online at https://academic.oup.com/aob and consist of the following.

Table S1: Δmalate, $\delta^{13}C$ values and structural traits in leaves of F_1 hybrids.

Table S2: structural traits of mesophyll cells and their chloroplasts in leaves of F_1 hybrids.

Figure S1: gross morphology of *C. ensifolium*, *C. bicolor* subsp. *pubescens* and their F_1 hybrids.

Figure S2: structural traits of mesophyll cells examined in this study.

Figure S3: structural traits of mesophyll chloroplasts examined in this study.

Figure S4: day/night changes in malate content in leaves of *C. ensifolium*, *C. bicolor* subsp. *pubescens* and their F_1 hybrids.

ACKNOWLEDGEMENTS

We thank Mr K. Suzuki for skilful care of the plants at Tsukuba Botanical Garden. The antisera for PEPC and PPDK were generously provided by Drs T. Sugiyama and H. Sakakibara, RIKEN, Yokohama, Japan. The antiserum for Rubisco LSU was a kind gift of the late Dr S. Muto, Nagoya University, Nagoya, Japan. O.U. conceived this study and T.Yu. produced the hybrid plants. Y.Y.H., M.O., Y.H., T.Ya. and O.U. conducted the experiments and analysed the data. O.U. wrote the manuscript, and all authors read and approved it. The authors declare that they have no conflict of interest.

FUNDING

This study was supported by the Japan Society for the Promotion of Science KAKENHI (JP 24370040).

LITERATURE CITED

Bang SW, **Ueno O**, **Wada Y**, **Hong SK**, **Kaneko Y**, **Matsuzawa Y. 2009**. Production of *Raphanus sativus* (C_3)-*Moricandia arvensis* (C_3-C_4 intermediate) monosomic and disomic addition lines with each parental cytoplasmic background and their photorespiratory characteristics. *Plant Production Science* **12**: 70–79.

Barrera-Zambrano VA, **Lawson T**, **Olmos E**, **Fernandez-Garcia N**, **Borland AM. 2014**. Leaf anatomical traits which accommodate the facultative engagement of crassulacean acid metabolism in tropical trees of the genus *Clusia*. *Journal of Experimental Botany* **65**: 3513–3523.

Beaulieu JM, **Leitch IJ**, **Patel S**, **Pendharkar A**, **Knight CA. 2008**. Genome size is a strong predictor of cell size and stomatal density in angiosperms. *New Phytologist* **179**: 975–986. doi:10.1111/j.1469-8137.2008.02528.x.

Björkman O. 1976. Adaptive and genetic aspects of C_4 photosynthesis. In: **Burris RH**, **Black CC**, eds. *CO_2 metabolism and plant productivity*. Baltimore: University Park Press, 287–309.

Björkman O, **Nobs M**, **Pearcy R**, **Boynton J**, **Berry J. 1971**. Characteristics of hybrids between C_3 and C_4 species of *Atriplex*. In: **Hatch MD**, **Osmond CB**, **Slatyer RO**, eds. *Photosynthesis and photorespiration*. New York: Wiley-Interscience, 105–119.

Borland AM, **Hartwell J**, **Weston DJ**, ***et al***. **2014**. Engineering crassulacean acid metabolism to improve water-use efficiency. *Trends in Plant Science* **19**: 327–338. doi:10.1016/j.tplants.2014.01.006.

Borland AM, **Leverett A**, **Hurtado-Castano N**, **Hu R**, **Yang X. 2018**. Functional anatomical traits of the photosynthetic organs of plants with crassulacean acid metabolism. In: **Adams WW III**, **Terashima I**, eds. *The leaf: a platform for performing photosynthesis*. Dordrecht: Springer, 281–305.

Brown RH, **Bouton JH. 1993**. Physiology and genetics of interspecific hybrids between photosynthetic types. *Annual Review of Plant Physiology and Plant Molecular Biology* **44**: 435–456.

Chollet R, **Vidal J**, **O'Leary MH. 1996**. Phosphoenolpyruvate carboxylase: a ubiquitous, highly regulated enzyme in plants. *Annual Review of Plant Physiology and Plant Molecular Biology* **47**: 273–298. doi:10.1146/annurev.arplant.47.1.273.

Cousins AB, **Mullendore DL**, **Sonawane BV. 2020**. Recent developments in mesophyll conductance in C_3, C_4, and crassulacean acid metabolism plants. *Plant Journal* **101**: 816–830. doi:10.1111/tpj.14664.

Cushman JC, **Bohnert HJ. 1999**. Crassulacean acid metabolism: molecular genetics. *Annual Review of Plant Physiology and Plant Molecular Biology* **50**: 305–332. doi:10.1146/annurev.arplant.50.1.305.

Cushman JC, **Agarie S**, **Albion RL**, **Elliot SM**, **Taybi T**, **Borland AM. 2008**. Isolation and characterization of common ice plant deficit in crassulacean acid metabolism. *Plant Physiology* **147**: 228–238. doi:10.1104/pp.108.116889.

Dever LV, **Boxall SF**, **Knerova J**, **Hartwell J. 2015**. Transgenic perturbation of the decarboxylation phase of crassulacean acid metabolism alters physiology and metabolism but has only a small effect on growth. *Plant Physiology* **167**: 44–59.

Dittrich P. 1976. Nicotinamide adenine dinucleotide-specific 'malic' enzyme in *Kalanchoe daigremontiana* and other plants exhibiting crassulacean acid metabolism. *Plant Physiology* **57**: 310–314. doi:10.1104/pp.57.2.310.

Dittrich P, **Wilbur WH**, **Black CC. 1973**. Phosphoenolpyruvate carboxykinase in plants exhibiting crassulacean acid metabolism. *Plant Physiology* **52**: 357–361.

Ehleringer JR, **Monson RK. 1993**. Evolutionary and ecological aspects of photosynthetic pathway variation. *Annual Review of Ecology and Systematics* **24**: 411–439. doi:10.1146/annurev.es.24.110193.002211.

Ehleringer JR, **Osmond CB. 1989**. Stable isotopes. In: **Pearcy PW**, **Ehleringer JR**, **Mooney HA**, **Randle PW**, eds. *Plant physiological ecology*. London: Chapman & Hall, 281–300.

Evans JR, **Loreto F. 2000**. Acquisition and diffusion of CO_2 in higher plant leaves. In: **Leegood RC**, **Sharkey TD**, **von Caemmerer S** eds. *Photosynthesis: physiology and metabolism*. Dordrecht: Kluwer Academic Publishers, 321–351.

Fioretto A, **Alfani A. 1988**. Anatomy of succulence and CAM in 15 species of *Senecio*. *Botanical Gazette* **149**: 142–152. doi:10.1086/337701.

Franks PJ, **Drake PL**, **Beerling DJ. 2009**. Plasticity in maximum stomatal conductance constrained by negative correlation between stomatal size and density: an analysis using *Eucalyptus globulus*. *Plant, Cell and Environment* **32**: 1737–1748. doi:10.1111/j.1365-3040.2009.02031.x.

Gibson AC. 1982. The anatomy of succulence. In: **Ting IP**, **Gibbs M**, eds. *Crassulacean acid metabolism: proceedings of the fifth annual symposium in botany*. Rockville MD: American Society of Plant Physiologists, 1–17.

Hatch MD. 1987. C_4 photosynthesis: a unique blend of modified biochemistry, anatomy and ultrastructure. *Biochimica et Biophysica Acta* **895**: 81–106.

Herrera A. 2020. Are thick leaves, large mesophyll cells and small intercellular air spaces requisites for CAM? *Annals of Botany* **125**: 859–868. doi:10.1093/aob/mcaa008.

Heyduk K, **Burrell N**, **Lalani F**, **Leebens-Mack J. 2016**. Gas exchange and leaf anatomy of a C_3–CAM hybrid, *Yucca gloriosa* (Asparagaceae). *Journal of Experimental Botany* **67**: 1369–1379. doi:10.1093/jxb/erv536.

Heyduk K, **Ray JN**, **Leebens-Mack J. 2021**. Leaf anatomy is not correlated to CAM function in a C_3+CAM hybrid species, *Yucca gloriosa*. *Annals of Botany* **127**: 437–449. doi:10.1093/aob/mcaa036.

Holtum JAM, **Osmond CB. 1981**. The gluconeogenetic metabolism of pyruvate during deacidification in plants with crassulacean acid metabolism. *Australian Journal of Plant Physiology* **8**: 31–44.

Hudson GS, **Mahon JD**, **Anderson PA**, ***et al***. **1990**. Comparisons of rbcL genes for the large subunit of ribulose bisphosphate carboxylase from closely related C_3 and C_4 plant species. *Journal of Biological Chemistry* **265**: 808–814. doi:10.1016/s0021-9258(19)40121-x.

Izui K, **Matsumura H**, **Furumoto T**, **Kai Y. 2004**. Phosphoenolpyruvate carboxylase: a new era of structural biology. *Annual Review of Plant Biology* **55**: 69–84. doi:10.1146/annurev.arplant.55.031903.141619.

Kondo A, **Nose A**, **Ueno O. 1998**. Leaf inner structure and immunogold localization of some enzymes involved in carbon metabolism in CAM plants. *Journal of Experimental Botany* **49**: 1953–1961. doi:10.1093/jxb/49.329.1953.

Kondo A, **Nose A**, **Yuasa H**, **Ueno O. 2000**. Species variation in the intercellular localization of pyruvate, Pi dikinase in leaves of crassulacean acid metabolism plants: an immunogold localization study. *Planta* **210**: 611–621. doi:10.1007/s004250050051.

Kondo A, **Kaikawa J**, **Funaguma T**, **Ueno O. 2004**. Clumping and dispersal of chloroplasts in succulent plants. *Planta* **219**: 500–506. doi:10.1007/s00425-004-1252-3.

Lujan M, **Oleas N**, **Winter K. 2022**. Evolutionary history of CAM photosynthesis in neotropical *Clusia*: insights from genomics, anatomy, physiology and climate. *Botanical Journal of the Linnean Society* **199**: 538–556.

Lüttge U. 2004. Ecophysiology of crassulacean acid metabolism (CAM). *Annals of Botany* **93**: 629–652. doi:10.1093/aob/mch087.

Males J. 2018. Concerted anatomical change associated with crassulacean acid metabolism in the Bromeliaceae. *Functional Plant Biology* **45**: 681–695. doi:10.1071/fp17071.

Maxwell K, **von Caemmerer S**, **Evans JR. 1997**. Is a low internal conductance to CO_2 diffusion a consequence of succulence in plants with crassulacean acid metabolism? *Australian Journal of Plant Physiology* **24**: 777–786.

Maxwell K, **Borland AM**, **Haslam RP**, **Helliker BR**, **Roberts A**, **Griffiths H. 1999**. Modulation of Rubisco activity during the diurnal phases of the crassulacean acid metabolism plant *Kalanchoë daigremontiana*. *Plant Physiology* **121**: 849–856. doi:10.1104/pp.121.3.849.

Möllering H. 1974. Determination of malate dehydrogenase and glutamate-oxaloacetate transaminase. In: **Bergmeyer HU,** ed. *Methods of enzymatic analysis*, Vol. **3**. New York: Academic Press, 1589–1593

Motomura H, **Yukawa T**, **Ueno O**, **Kagawa A. 2008**. The occurrence of crassulacean acid metabolism in *Cymbidium* (Orchidaceae) and its ecological and evolutionary implications. *Journal of Plant Research* **121**: 163–177. doi:10.1007/s10265-007-0144-6.

Nelson EA, **Sage RF. 2008**. Functional constrains of CAM leaf anatomy: tight cell packing is associated with increased CAM function across a gradient of CAM expression. *Journal of Experimental Botany* **59**: 1841–1850. doi:10.1093/jxb/erm346.

Nelson EA, **Sage TL**, **Sage RF. 2005**. Functional leaf anatomy of plants with crassulacean acid metabolism. *Functional Plant Biology* **32**: 409–419. doi:10.1071/fp04195.

Nimmo HG. 2000. The regulation of phosphoenolpyruvate carboxylase in CAM plants. *Trends in Plant Science* **5**: 75–80. doi:10.1016/s1360-1385(99)01543-5.

Oakley JC, **Sultmanis S**, **Stinson CR**, **Sage TL**, **Sage RF. 2014**. Comparative studies of C_3 and C_4 *Atriplex* hybrids in the genomics era: physiological assessments. *Journal of Experimental Botany* **65**: 3637–3647. doi:10.1093/jxb/eru106.

Ogura-Tsujita Y, **Miyoshi K**, **Tsutsumi C**, **Yukawa T. 2014**. First flowering hybrid between autotrophic and mycoheterotrophic plant species: breakthrough in molecular biology of mycoheterotrophy. *Journal of Plant Research* **127**: 299–305. doi:10.1007/s10265-013-0612-0.

Osmond CB. 1978. Crassulacean acid metabolism: a curiosity in context. *Annual Review of Plant Physiology* **29**: 379–414. doi:10.1146/annurev.pp.29.060178.002115.

Roberts A, **Borland AM**, **Griffiths H. 1997**. Discrimination processes and shifts in carboxylation during the phases of crassulacean acid metabolism. *Plant Physiology* **113**: 1283–1292. doi:10.1104/pp.113.4.1283.

Sato R, **Suzuki Y. 2010**. Carbon and nitrogen stable isotope analysis by elemental analyzer/isotope ratio mass spectrometer (EA/IRMS). *Research of Organic Chemistry* **26**: 21–29.

Schiller K, **Bräutigam A. 2021**. Engineering of crassulacean acid metabolism. *Annual Review of Plant Biology* **72**: 77–103. doi:10.1146/annurev-arplant-071720-104814.

Silvera K, **Santiago LS**, **Winter K. 2005**. Distribution of crassulacean acid metabolism in orchids of Panama: evidence of selection for weak and strong modes. *Functional Plant Biology* **32**: 397–407. doi:10.1071/fp04179.

Silvera K, **Winter K**, **Rodriguez BL**, **Albion RL**, **Cushman JC. 2014**. Multiple isoforms of phosphoenolpyruvate carboxylase in the Orchidaceae (subtribe Oncidiinae): implications for the evolution of crassulacean acid metabolism. *Journal of Experimental Botany* **65**: 3623–3636. doi:10.1093/jxb/eru234.

Simpson CJC, **Reeves G**, **Tripathi A**, **Singh P**, **Hibberd JM. 2022**. Using breeding and quantitative genetics to understand the C_4 pathway. *Journal of Experimental Botany* **73**: 3072–3084. doi:10.1093/jxb/erab486.

Stata M, **Sage TL**, **Rennie TD**, ***et al***. **2014**. Mesophyll cells of C_4 plants have fewer chloroplasts than those of closely related C_3 plants. *Plant, Cell and Environment* **37**: 2587–2600. doi:10.1111/pce.12331.

Takao K, **Shirakura H**, **Hatakeyama Y**, **Ueno O. 2022**. Salt stress induces Kranz anatomy and expression of C_4 photosynthetic enzymes in the amphibious sedge *Eleocharis vivipara*. *Photosynthesis Research* **153**: 93–102. doi:10.1007/s11120-022-00913-y.

Teeri JA, **Overton J. 1981**. Chloroplast ultrastructure in two crassulacean species and an F1 hybrid with differing biomass $\delta^{13}C$ values. *Plant, Cell and Environment* **4**: 427–431. doi:10.1111/1365-3040.ep11604660.

Töpfer N, **Braam T**, **Shameer S**, **Ratcliffe RG**, **Sweetlove LJ. 2020**. Alternative crassulacean acid metabolism modes provide environment-specific water-saving benefits in a leaf metabolic model. *Plant Cell* **32**: 3689–3705. doi:10.1105/tpc.20.00132.

Tsutsumi N, **Tohya M**, **Nakashima T**, **Ueno O. 2017**. Variations in structural, biochemical and physiological traits of photosynthesis and resource use efficiency in *Amaranthus* species (NAD-ME-type C_4). *Plant Production Science* **20**: 300–312. doi:10.1080/1343943x.2017.1320948.

Ueno O. 1998. Immunogold localization of photosynthetic enzymes in leaves of various C_4 plants, with particular reference to pyruvate, orthophosphate dikinase. *Journal of Experimental Botany* **49**: 1637–1646. doi:10.1093/jxb/49.327.1637.

Ueno O, **Bang SW**, **Wada Y**, ***et al***. **2003**. Structural and biochemical dissection of photorespiration in hybrids differing in genome constitution between *Diplotaxis tenuifolia* (C_3-C_4) and radish (C_3). *Plant Physiology* **132**: 1550–1559. doi:10.1104/pp.103.021329.

Winter K. 1985. Crassulacean acid metabolism. In: **Barber J**, **Baker NR**, eds. *Photosynthetic mechanisms and the environment*. Amsterdam: Elsevier, 329–387.

Winter K. 2019. Ecophysiology of constitutive and facultative CAM photosynthesis. *Journal of Experimental Botany* **70**: 6495–6508. doi:10.1093/jxb/erz002.

Winter K, **Holtum JAM. 2002**. How closely do the $\delta^{13}C$ values of crassulacean acid metabolism plants reflect the proportion of CO_2 fixed during day and night? *Plant Physiology* **129**: 1843–1851. doi:10.1104/pp.002915.

Winter K, **Smith JAC. 2022**. CAM photosynthesis: the acid test. *New Phytologist* **233**: 599–609.

Winter K, **Aranda JE**, **Holtum JAM. 2005**. Carbon isotope composition and water-use efficiency in plants with crassulacean acid metabolism. *Functional Plant Biology* **32**: 381–388. doi:10.1071/fp04123.

Yabiku T, **Ueno O. 2017**. Variations in physiological, biochemical, and structural traits of photosynthesis and resource use efficiency in maize and teosintes (NADP-ME-type C_4). *Plant Production Science* **20**: 448–458. doi:10.1080/1343943x.2017.1398050.

Yang X, **Cushman JC**, **Borland AM**, ***et al***. **2015**. A roadmap for research on crassulacean acid metabolism (CAM) to enhance sustainable food and bioenergy production in a hotter, drier world. *New Phytologist* **207**: 491–504. doi:10.1111/nph.13393.

Yuan G, **Hassan MM**, **Liu D**, ***et al***. **2020**. Biosystems design to accelerate C_3-to-CAM progression. *BioDesign Research* **2020**: 3686791.

Yukawa T, **Stern WL. 2002**. Comparative vegetable anatomy and systematics of *Cymbidium* (Cymbidieae: Orchidaceae). *Botanical Journal of the Linnean Society* **138**: 383–419. doi:10.1046/j.1095-8339.2002.00038.x.

Yukawa T, **Miyoshi K**, **Yokoyama J. 2002**. Molecular phylogeny and character evolution of *Cymbidium* (Orchidaceae). *Bulletin of the National Science Museum Tokyo Series B* **18**: 129–139.